Molecular Crystals and Liquid Crystals

ISSN: 1542-1406 (Print) 1563-5287 (Online) Journal homepage: http://www.tandfonline.com/loi/gmcl20

Electrical and structural analysis of $xPbO-(1-x)B_2O_3$ ($0.3 \leq x \leq 0.9$) glasses

N. Ait Hana, J. Aride, M. Haddad, K. Benkhouja, B. Sahraoui & M. Taibi

To cite this article: N. Ait Hana, J. Aride, M. Haddad, K. Benkhouja, B. Sahraoui & M. Taibi (2016) Electrical and structural analysis of $xPbO-(1-x)B_2O_3$ ($0.3 \leq x \leq 0.9$) glasses, Molecular Crystals and Liquid Crystals, 627:1, 106-117, DOI: 10.1080/15421406.2015.1137125

To link to this article: http://dx.doi.org/10.1080/15421406.2015.1137125

Published online: 13 May 2016.

MOL. CRYST. LIQ. CRYST.
2016, VOL. 627, 106–117
http://dx.doi.org/10.1080/15421406.2015.1137125

Taylor & Francis
Taylor & Francis Group

Electrical and structural analysis of xPbO-(1-x)B_2O_3 ($0.3 \leq x \leq 0.9$) glasses

N. Ait Hana[a], J. Aride[a], M. Haddad[b], K. Benkhouja[c], B. Sahraoui[d], and M. Taibi[a]

[a]Université Mohammed V, LPCMIO, Ecole Normale Supérieure, Rabat, Morocco; [b]LASMAR, URAC11, Faculté des Sciences, Université Moulay Ismail Meknès Maroc; [c]E2M LCCA, Faculté des Sciences, Université Chouaib Doukkali El Jadiada Maroc; [d]Institute of Sciences and Molecular Technologies of Angers - UMR CNRS 6200, ANGERS cedex2

ABSTRACT

Different xPbO–(1–x)B_2O_3 glasses were prepared by conventional melting method. They were investigated by differential scanning calorimetry (DSC), Raman and IR spectroscopy. The glasse's structure and the PbO role to the formation of the borate units in the framework is investigated. The dielectric constant and dielectric loss were measured at different frequencies and as a function of the temperature. The electrical measurements carried out showed semiconductor behavior of the conductivity as a function of temperature. The activation energies (Ea) for the conduction process indicated a thermally activated hopping mechanism. The calculated Ea values are typically 0.67–2.46 eV.

KEYWORDS

borate; glasses; dielectric properties; IR spectroscopy

1. Introduction

In the last few years, there has been an enormous amount of research on improving the physical properties of borate glasses by introducing a number of glass formers and modifiers such as TiO_2, V_2O_5, Al_2O_3, MoO_3, Ta_2O_3, Sb_2O_3, As_2O_3 etc., into B_2O_3 glass network. The investigation on the physical properties of glass containing a glass former B_2O_3 along with modifiers (alkali oxides) is an extremely interesting subject of study. The large interest concerning this material is motivated by their high ionic conductivity and numerous applications such as: biomaterials with antibacterial and antimicrobial effects, biomaterials for cancer, chemical sensors, electrochromic display devices and solid batteries [1–11].

The basic units of pure borate glasses are trigonal BO_3 groups, the addition of a modifier to borate networks has different effects. In borate network, some studies prove that the addition of a PbO could act both as a glass network former and as modifier depending on its concentration in the glasses [3,7]. Raman studies on some ternary lead borate glasses suggest that PbO may get incorporated into the network in four coordinated positions since the boron atoms in these glasses are both three (BO_3) and four coordinated (BO_4) [12]. A variety of anionic borate species such as penta-, tri-, tetra-, di-, pyro-, ortho-borate besides structural entities like boroxol ring have been identified in glasses containing B_2O_3 and PbO [12,13]. Of course the concentration of these borate species in the glass structure is given by the nature and concentration of modifier oxide.

CONTACT M. Taibi taibiens@yahoo.fr Mohammed V University, LPCMIO, ENS, BP 5118 Takaddoum, Rabat, Morocco
Color versions of one or more of the figures in the article can be found online at www.tandfonline.com/gmcl.

In the present work, we propose to add PbO to B_2O_3 for establish aspects related to the preparation conditions and structure of PbO-B_2O_3 glasses by means of two complementary spectroscopic methods: infrared absorption and Raman scattering. These two powerful methods provide useful information concerning the short-range order in these glasses.

2. Experimental procedure

For this study we have chosen the following composition $xPbO–(1–x)B_2O_3$ with x ranging from 0,3 to 0,9 (in mol %). Analytical grade reagents of H_3BO_3 and PbO powders in appropriate amounts were thoroughly mixed in an agate mortar, heated at about 200°C for 24 h in a platinum crucible. The mixtures were annealed progressively to 500°C. The resulting compound is ground again and melted (between 750 and 900°C, depending of PbO content) and then cooled on a metal plate preheated at 200°C. The obtained glasses are homogenous and transparent. The amorphous state of the samples and the products of crystallization were characterized by XRD technique (Siemens D500 X-ray diffractometer employing Cu Kα radiation).

Thermal studies were carried out using a differential scanning calorimetry (DSC) type SETARAM 121 under argon atmosphere at a flow of 50 ml/min.. The measurements were conducted at heating rate 10°C/min) using about 20 mg of glass powder in a Pt crucible. The variation in the amount of sample used for crystallization studies was within $\pm$ 0, 1 mg.

The infrared spectra of glasses were recorded at room temperature using KBr disc technique. A Tensor 27 FTIR Bruker spectrometer was used to obtain the spectra in the wave number range 400 and 4000 cm^{-1}.

Raman spectra were measured at room temperature with a Renishaw micro-Raman spectrometer (RM1000) equipped with a CCD detector, a 1800 gr/mm grating and an external Leica DMLM confocal microscope. The excitation source is a He–Ne laser (19mW) operating at 632.8nm. The laser spot was focused on the sample surface using either 50x or 100x objectives. Raman spectra were collected on numerous spots on the sample and recorded with Peltier cooled CCD Camera. The spectra were measured between 100 and 2000 cm^{-1}.

The electrical measurements on the glass samples were carried out using a specially designed vacuum cell. Two silver electrodes were deposited onto the samples, the flat surfaces of the glass samples were painted with silver paste. The different electrical measurements were performed using a LCR meter type HP 4284A opering from 20 Hz to 1MHz.

3. Results and discussion

XRD analysis was used in to ensure that no crystallization occurred during the solidification of the elaborated samples. The results confirmed that the samples were free of crystals as evidenced in Figure 1.

3.1. *Thermal analysis*

The DSC curves from the different samples at heating rate b = 10°C.min^{-1} were indicated in Figures 2 and 3. Values of characteristic temperatures are summarized in Table 1. T_g was the inflection temperature of glass transition, T_c was the crystallization temperature and T_f was the peak point of endothermic peak for melting. The observation of glass transition temperature T_g by DSC and the amorphous state by XRD confirmed the glassy nature of the samples. When the content of $50 \leq PbO \leq 70$ mol%, both exothermic and endothermic peaks

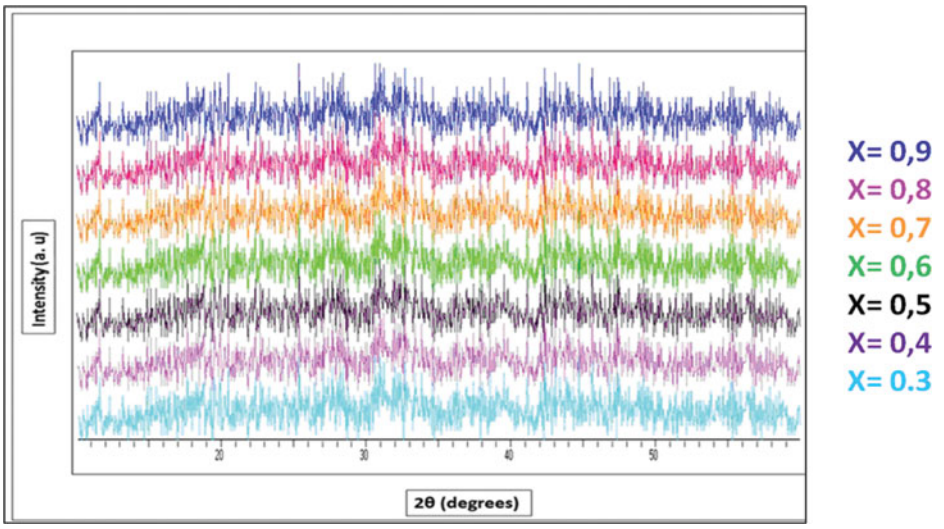

Figure 1. XRD patterns of xPbO-(1-x)B_2O_3 (0.3 ≤ x≤ 0.9) glasses.

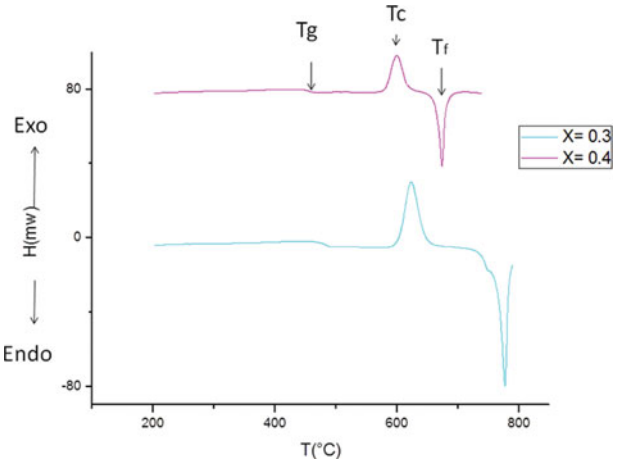

Figure 2. DSC curves for xPbO-(1-x)B_2O_3 (0.3≤ x≤ 0.4) glasses at heating rate b = 10°C.min^{-1}

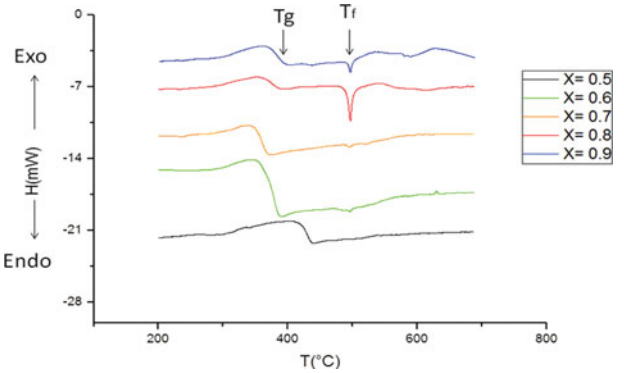

Figure 3. DSC curves of xPbO-(1-x)B_2O_3 (0.5≤ x≤ 0.9) glasses at heating rate b = 10°C.min^{-1}

Table 1. Thermal parameters of xPbO–(1–x)B_2O_3 glass system.

composition	T_g (°C)	T_c (°C)	T_f (°C)
x = 0,3	478	623	777
x = 0,4	453	599	674
x = 0,5	428	—-	—-
x = 0,6	373	—-	—-
x = 0,7	360	—-	—-
x = 0,8	376	—-	496
x = 0,9	383	—-	496

are not observed, which is due to the crystallization during cooling process. It is well known that crystallized glasses, relatively stabilized, have no exothermal and endothermal changes during heating treatments. In the region of PbO ≥ 80 mol%, there is no any exothermic peak observed, indicating that glasses in this composition region are stable on heating against crystallization [1,2].

The compositional dependence of glass transition temperature is shown in Figure 4. It is observed that glass transition temperature varies non-linearly with x. The T_g is found to decrease from x = 0.3 up to x = 0.7 and after this composition, T_g increases. The T_g behaviour with x mol% is described in the following, based on the network modifications evidenced from IR and Raman spectroscopy.

The increase in the T_g in general may be due to small decrease in the number of non-bridging oxygen ions and is also associated with the formation and minor variation of BO_4 tetrahedral which serve to cross-link the network by covalent B-O bonds [1,3,5]. In the present study the non-linear variation of T_g with x is due to the creation and variation in the number of BO_3 triangular units, BO_4 tetrahedral units and to some extent bridging and non-bridging oxygen ions[4,11].

3.2. *Infrared spectroscopy*

The infrared spectra of xPbO-(1-x)B_2O_3 borate glasses are shown in Figure 5. Table 2 reportes FTIR results for all studied glasses. For lead borate glasses, the main peaks and assigned

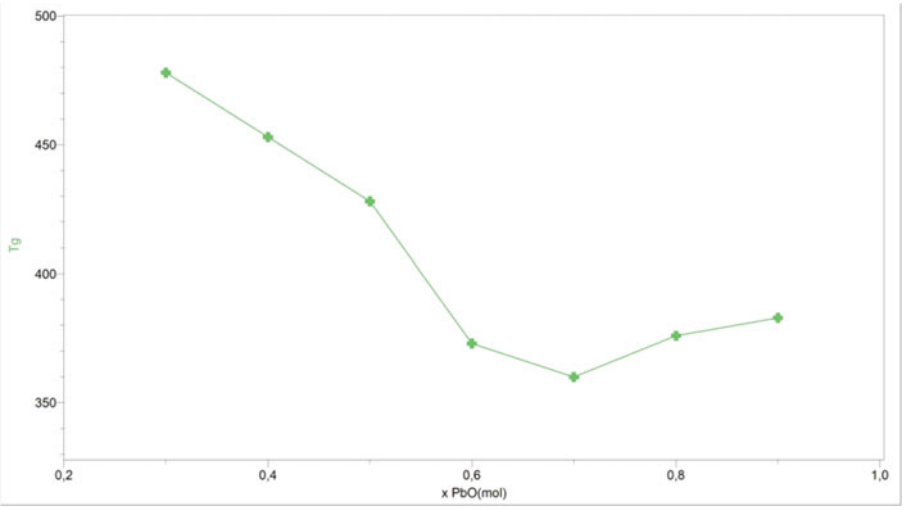

Figure 4. Variation of the glass transition Tg for xPbO-(1-x)B_2O_3 (0.3≤ x≤ 0.9) glasses at heating rate b = 10°C.min^{-1}

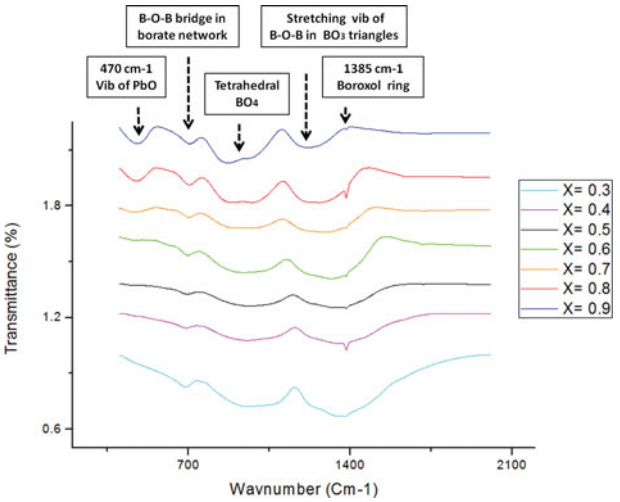

Figure 5. Infrared absorption spectra of xPbO-(1-x)B_2O_3 (0.3≤ x≤ 0.9) glasses.

vibration types can be summarized υ_{as} B–O stretching in BO_3 groups at1400–1380 cm^{-1} [4,6,7], stretching vibrations of oxygens bridging trigonal borons at 1230–1160 cm^{-1}[5–7], B–O stretching modes of BO_4 groups at 1080–1000 cm^{-1} and 890–840 cm^{-1}[8,9], bending of B–O–B in BO_3 groups at 710–680 cm^{-1} [7, 21] and bending vibration frequency of Pb–O at 480–460 cm^{-1} [1,10,11]. With the introduction of PbO up to 0.9 mol%, the intensity of the band due to BO_4 units is observed to increase while that of BO_3 units is observed to decrease. The band due to tetrahedral PbO_4 units is observed for the glasses 0.5PbO–0.5B_2O_3 to 0.9PbO–0.1B_2O_3 and the intensity of this band is also increased with the concentration PbO.

It is well known that the effect of introduction of modifier ions into B_2O_3 glass converts sp2 planar BO_3 units into more stable sp3 tetrahedral BO_4 units and may also create non bridging oxygens. Each BO_4 unit is linked to two such other units and one oxygen from each unit with a metal ion and the structure leads to the formation of long tetrahedron chains [9,18]. PbO is in general a glass modifier and enters the glass network, by breaking up the B–O–B bonds (normally the oxygen's of PbO break the local symmetry while Pb^{2+} ions occupy interstitial positions) and introduces coordinated defects known as dangling bonds along with non-bridging oxygen ions. In this case Pb^{2+} is tetrahedral coordinated [8,11]. PbO may also participate in the glass network with PbO_4 structural units when lead ion is linked to four oxygens in a covalency bond configuration. In such a case the network structure is considered to build up from PbO_4 units [10, 12] and alternate with BO_4 structural units and may form

Table 2. Observed and attribution of IR absorption bands in PbO–B_2O_3 glass system.

Glass sample	δ s Pb–O [PbO4]	δ B–O–B [BO3]	υ_{as} B–O [BO4]	υ_a B–O [BO4]	υ_a B–O [BO3] in boroxol ring	υ_{as} B–O [BO3]	
X = 0.3	—–	685	955	1075	1235	1324	1386
X = 0.4	—–	692	947	1076	1221	1316	1386
X = 0.5	463	695	974		1226	1323	1386
X = 0.6	465	696	915	1034	1223	1321	1386
X = 0.7	468	700	910	1021	1239	1317	1386
X = 0.8	472	702	886	983	1227	1289	1386
X = 0.9	476	704	873	994	1221	—–	1386

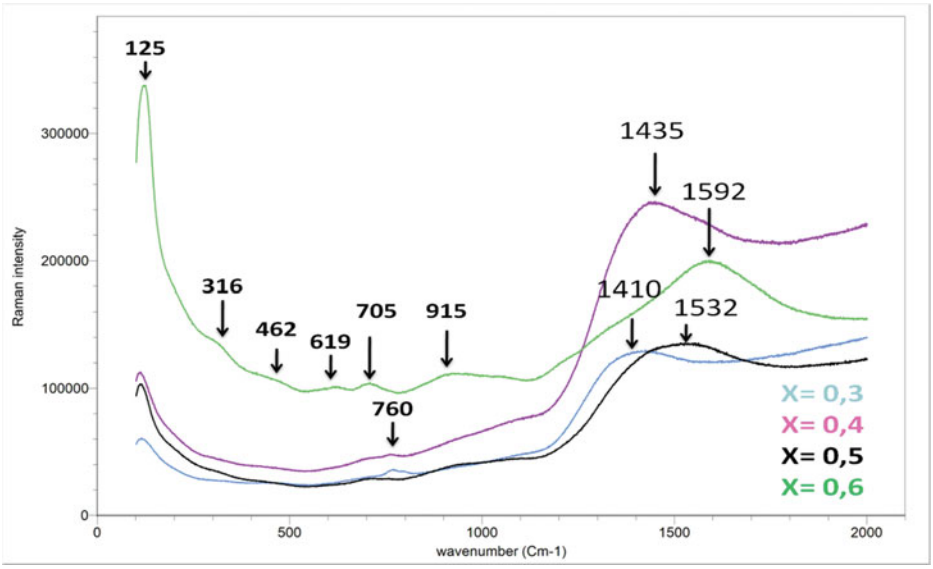

Figure 6. Raman spectra of xPbO-(1-x)B_2O_3 ($0.3 \leq x \leq 0.6$) glasses.

the linkages of the type Pb–O–B. The presence of such PbO_4 units is evident from the band in the IR spectra at above 475 cm^{-1}.

3.3. *Raman spectroscopy*

The Raman spectra of xPbO–(1–x)B_2O_3 borate glass system with x = 0.3, 0.4, 0.5 and 0.6 mol%, are shown in Figure 6. The analysis of the Raman spectra reveals the following points:

- √ The bands in the range of 1410–1592 cm^{-1} are due to the B—O stretching vibrations in various configurations of borate groups [12].
- √ The peak at 920 cm^{-1} is due to pentaborate and tetraborate groups [12–13].
- √ The peak at 760 cm^{-1} which appears for x = 0.3 and 0.4 due to ring breathing vibration of six membered ring containing both BO_3 triangles [17].
- √ Broad peaks in the range of 619–708 cm^{-1} are assigned to metaborate and diborate units, that is, ring typed metaborate peaking at 619 cm^{-1} [13–14] and chain typed metaborate at 708 cm^{-1} [16–18].
- √ The peaks at 462 cm^{-1} due to isolated diborate groups, Pb-O bond vibrations [15–16].
- √ The peak about 316 cm^{-1}, is assigned to B-O-Pb vibrational modes in different borate surroundings [14,17]
- √ The peak at 120 cm^{-1}, which is assigned to Pb-O vibrations either in PbO_4 square pyramids or in PbO_3 trigonal pyramids [17,18,23].

It is evident that with an increase in x both the "borate" parts of the network are changing significantly. It is clearly observed for x = 0.6 that has more bands to other simples.

The bands in the range of 1410–1592 cm^{-1} are due to the B—O stretching vibrations in various configurations of borate groups [12]. We observed in this region the peak positions for the simples were shifted to the high wavenumbers with a rise of PbO concentration.

In the region 120–500 cm^{-1} we observed three bands due to Pb-O vibrations. The band at 125 cm^{-1} present for all simples, which is assigned to Pb-O vibrations either in PbO_4 square

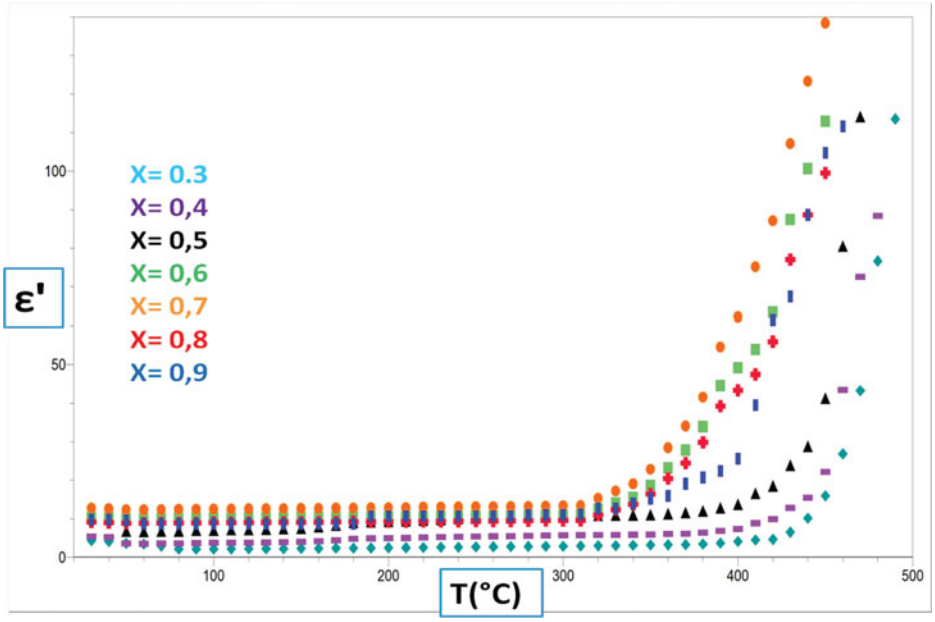

Figure 7. Variation of dielectric constant ε' with temperature at 10 Hz of xPbO-(1-x)B_2O_3 ($0.3 \leq x \leq 0.9$) glasses.

pyramids or in PbO_3 trigonal pyramids [17,18,23], We can see the intensity of this band increased with increasing in PbO content up to 60 mol%. The bands at 316 and 462 cm^{-1} only for x = 0.6 which are assigned respectively to the B-O-Pb vibrational modes in different borate surroundings [14–17]. And to the isolated diborate groups, Pb-O bond vibrations [15–16]. The peak at 760 cm-1 which appears for x = 0.3 and 0.4 due to ring breathing vibration of six membered ring containing both BO_3 triangles [17]. The absence of this peak in the simples x = 0.5 and x = 0.6 give in return three bands at 619 and 708 cm^{-1} which assigned to metaborate and diborate units, that is, ring typed metaborate peaking at 619 cm^{-1} [13–14] and chain typed metaborate at 708 cm-1 [16–18], and the band at 920 cm^{-1} due to pentaborate and tetraborate group [12–13]. These results obtained from Raman spectroscopy indicate that with the increase in the concentration of PbO in the glass matrix, B_2O_3 network convert the sp2 planar BO_3 into more stable sp3 tetrahedral BO_4, in agreement with the results of infrared spectroscopy, confirms the network structure of the glass is led to be broken with the addition of PbO and characterized by the borate anions.

3.4. *Electrical measurements*

The dielectric constant (ε), and conductivity (σ_{ac}) were calculated using the following expressions: $\varepsilon' = Cd/\varepsilon_o S$ (1), $\sigma_{ac}(\omega) = \omega\varepsilon'\varepsilon_o \tan\delta$ (2) where C measured capacitance of the sample (F), d thickness of the sample (m), ε_o permittivity of free space equals $8.85.10^{-12}$ $F.m^{-1}$, S the sample surface area (m^2), ω the angular frequency, tan δ the dielectric losses which is obtained directly from the instrument. The activation energies (Ea) were obtained by using the Arrhenius expression $\sigma_{ac} = \sigma_0 \exp(-Ea/kT)$ (3) [20,33].

Ea is the activation energy, k is the Boltzmann's constant, T is the absolute temperature and σ_0 is the temperature dependent pre-exponential factor.

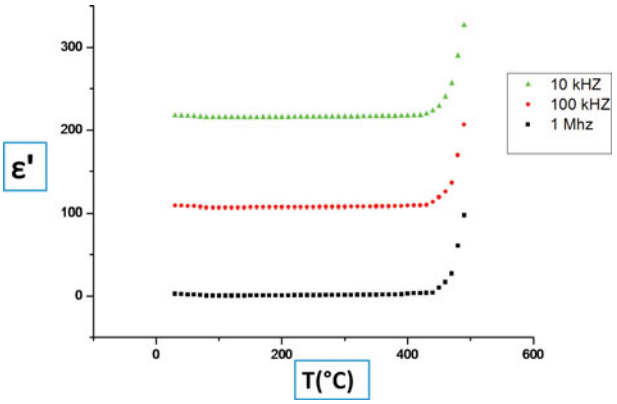

Figure 8. Variation of dielectric constant ε' with temperature at different frequencies of $0.3PbO–0.7B_2O_3$ glass.

3.3.1. *Dielectric constant and dielectric loss*

Figure 7 represents the temperature dependence of dielectric constant ε' at 10 kHz of xPbO–(1−x) B_2O_3 glasses and the dependence of ε', with temperature at different frequencies for the $0.3PbO–0.7B_2O_3$ glass is shown in Figure 8. It is observed that the dielectric constants of the present glasses decrease lightly with an increase of frequency and The value of ε', exhibits a considerable increase at higher temperatures; the rate of increase of ε', with temperature at any frequency is found to increase with the concentration of Pb^{2+} ions up to 0.7 mol% PbO and then decrease for 0.8 and 0.9 PbO mol% in the glass. The observed variation of dielectric constant ε' with temperature indicate that the present glasses are charge transfer type insulators in nature and that considerable tuning of dielectric properties could be achieved by adaptation the Pb^{2+} concentration in the glass matrix. [19,21,34]. The basis for this argument can be cited from the results of IR and Tg studies, which have indicated that the effect may be due to the reduction in the degree of disorder of the glass network when the concentration of Pb^{2+} ion increases from 0.7 to 0.9 PbO mol%.

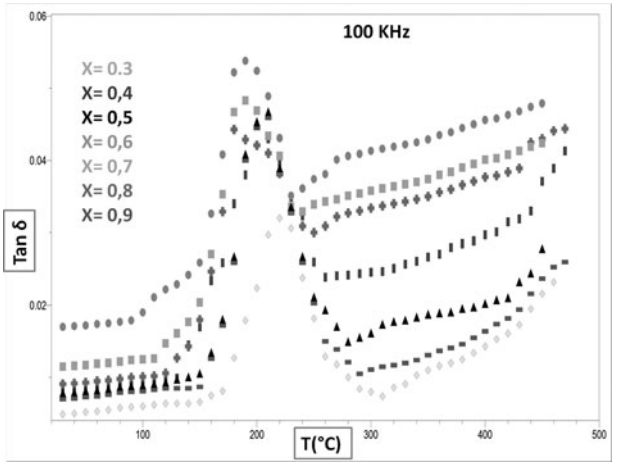

Figure 9. The comparison plot of variation of tanδ with temperature at 100 kHz for xPbO-(1-x)B_2O_3 ($0.3 \leq x \leq 0.9$) glasses.

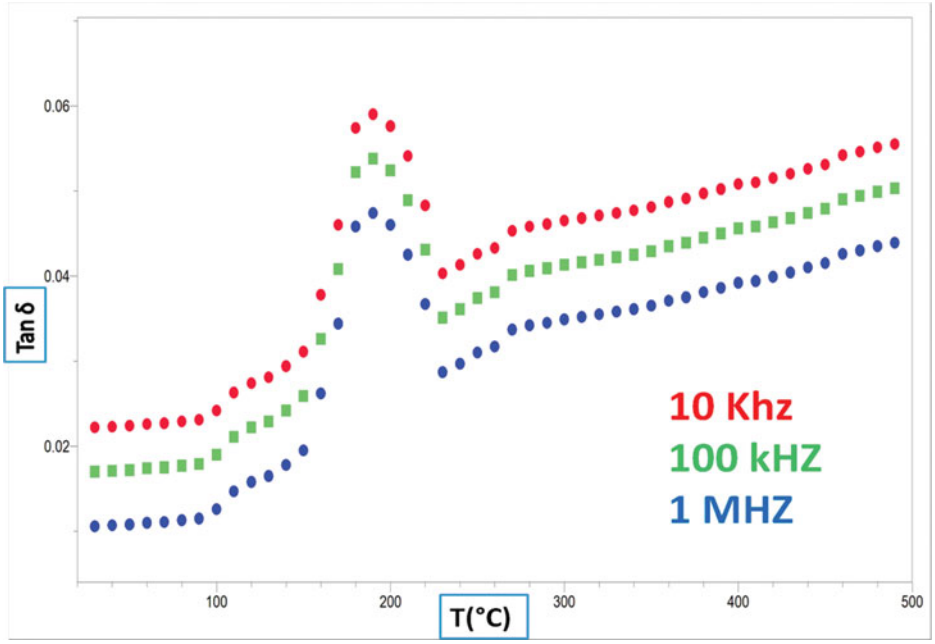

Figure 10. The comparison plot of variation of tanδ with temperature at different frequencies for 0.7PbO–30 B_2O_3 glass.

The variation of the dielectric loss, tanδ, with temperature, measured at a frequency of 100 kHz for xPbO–(1−x)B_2O_3 glasses and the temperature dependence of tanδ of 0.7PbO–30B_2O_3 glass at different frequencies are presented in Figures 9 and 10. The values of tanδ_{max} and the temperature region of relaxation are listed in Table 3.

From these figures we can see that the variation of the dielectric loss with temperature is the same as the variation of constant dielectric, i.e. the dielectric loss, tanδ, of the present glasses decreases slightly with an increase of frequency and also it increases with the concentration of Pb^{2+} ions up to 0.7 mol% PbO and then decreases for 0.8 and 0.9 PbO mol% in the glass.

The curves have exhibited distinct maxima; with increasing frequency, the temperature maximum shifts towards higher temperature and with increasing temperature the frequency maximum shifts towards higher frequency, indicating the dielectric relaxation character of dielectric losses of these glasses[23–25]. The relaxation effects in the studied glasses can be attributed to the Pb^{2+} complexes that possess net dipole moment [26, 27].

Table 3. Temperature region of relaxation and tanδ_{max} for xPbO–(1–x)B_2O_3 (0.3 ≤ x≤ 0.9) glasses.

	tanδ_{max}			Temp. region of relaxation(±1)°C		
Sample	10kHZ	100kHZ	1MHZ	10kHZ	100kHZ	1MHZ
X = 0.3	0.0373	0.0321	0.0287	170–310	170–310	170–310
X = 0.4	0.0513	0.0460	0.0394	150–290	150–290	150–290
X = 0.5	0.0520	0.0468	0.0415	140–280	140–280	140–280
X = 0.6	0.0537	0.0484	0.0419	110–240	110–240	110–240
X = 0.7	0.0591	0.0540	0.0476	90–230	91–232	92–231
X = 0.8	0.0494	0.0445	0.0377	120–250	120–251	122–250
X = 0.9	0.0500	0.0448	0.0379	130–260	131–259	132–261

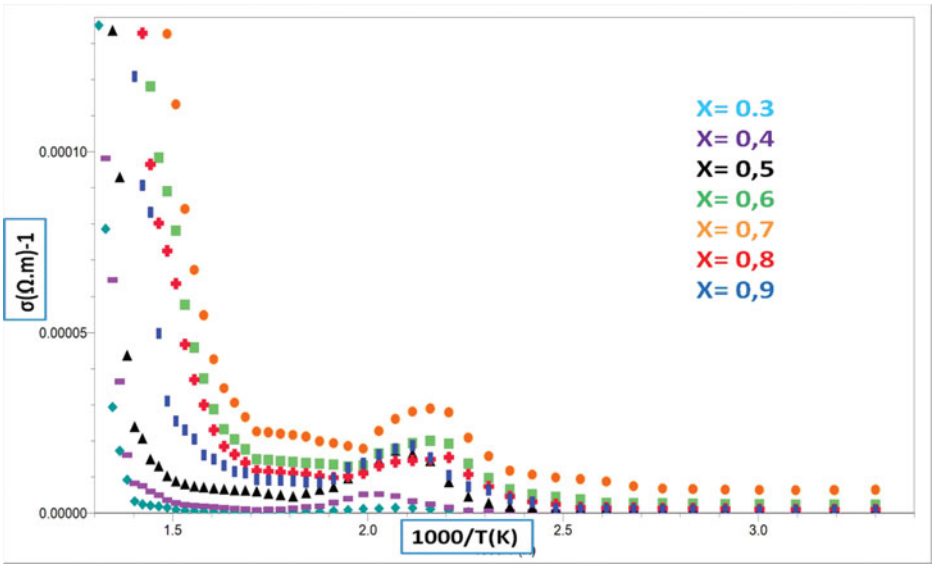

Figure 11. Variation of ac conductivity with 1000/T (K) at 1 MHz for xPbO-(1-x)B_2O_3 (0.3 ≤ x≤ 0.9) glasses.

3.3.2. *AC conductivity (σ_{ac}) and activation energy (Ea)*

Figure 11 shows the AC conductivity plots of xPbO–(1−x)B_2O_3 (0.3≤ x≤ 0.9) glass samples at 1 MHz. The conductivity AC is found to increase considerably with increase in the concentration of PbO at any given frequency and temperature up to 0.7 mol% PbO and then decreases for 0.8 and 0.9 PbO mol% doped glass. From these plots, the activation energy Ea for the conduction in the high temperature region over which a near linear dependence of log σ_{ac} with 1000/T could be observed in figure 12. This observation suggests the conductivity enhancement is directly related to the increasing mobility of the charge carriers in the high temperature region [28–31]. Further, the high temperature conductivity decreases in the concentration of PbO (from 0.7 to 0.9 mol %) and increases in the region (from 0.3 to 0.7 mol %). The decreasing trend of conductivity up to 0.9 mol% suggests that the conductivity is

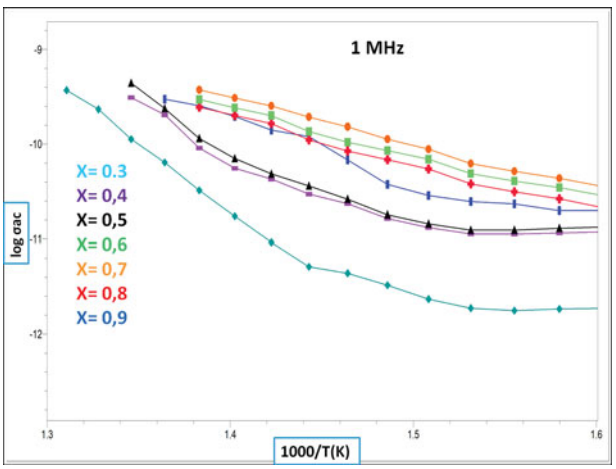

Figure 12. Variation of logσ_{ac} conductivity with 1000/T (K) at 1 MHz for xPbO–(1–x)B_2O_3 (0.3 ≤ x≤ 0.9) glasses.

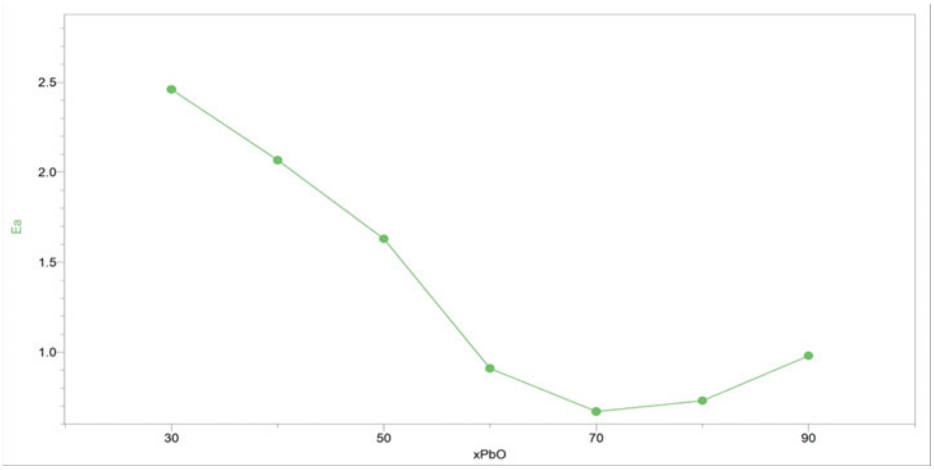

Figure 13. Variation of activation energy for xPbO-(1-x)B_2O_3 (0.3≤ x≤ 0.9) at 10 kHZ.

related to ionic motion, whereas in the other region, the conductivity seems to be related with electronic motion [22,30,32].

The variation of the activation energy as a function of the composition of PbO mol% is shown in Figure 13. The activation energy is found to decrease with increase of PbO content up to 0.7 PbO mol% and then increases for 0.8 and 0.9 PbO mol% doped glasses. One of the possible explanations for such a behavior is that the entry of Pb^{2+} ions into the network forming tetrahedral positions reduces the concentration of dangling bonds in the glass network since some of BO_4 structural units cross-link with PbO_4 and BO_4 units [28]. Because of increasing concentration of Pb^{2+} ions; these ions act as modifiers and generate bonding defects. The defects thus produced create easy pathways for the migration of charges that would build up space charge polarization leading to an increase in the dielectric parameters [30–31]. The most values of the dielectric parameters observed for glass x = 0.7 is obviously owing to the presence of Pb^{2+} that create disorder in the glass network. The increase of activation energy 0.8 and 0.9 PbO mol% may be attributed to association of Pb^{2+} ions with a pair of BO_4 groups (which exhibit the vibrational bands in the high frequency side of borate vibrational region) [22–30]. This observation suggests that the conductivity enhancement is directly related to the increasing mobility of the charge carriers in the high-temperature region.

We can note that the variation of the activation energy exhibit the same behavior that the variation of the glass temperature (Tg) versus the composition. This effect confirms that PbO content take the same role on the stability and on the conduction mode in the glasses.

4. Conclusion

In this paper, lead borate glasses have been synthesized and characterized along the series xPbO–(1–x)B_2O_3 (0.3 ≤ x≤ 0.9). Thermal, spectroscopic and electrical properties of the glasses are reported. AC electrical conductivity and in activation energy was calculated.

The summary of conclusions drawn from the study of various properties of PbO–B_2O_3 glasses is as follows:

- √ Homogeneous glasses of xPbO–(1–x)B_2O_3 (0.3 ≤ x≤ 0.9). glass system have been prepared by melt quench technique. The amorphous state of the prepared glasses was confirmed by X-ray diffraction.

- √ DSC measurements were carried out to determine the glass transition temperature (Tg) of the glass samples. Tg is found to decrease with x depicting a minimum at x = 0.7 mol% and there-after increases for 0.8 and 0.9 PbO mol%.
- √ The Raman and IR spectral investigations indicate that with the increase in the concentration of PbO in the glass matrix, B_2O_3 network convert the sp2 planar BO_3 into more stable sp3 tetrahedral BO_4.
- √ The dielectric parameters ε', tan δ and σ_{ac} are found to increase with temperature; while the dielectric breakdown strength and the activation energy for AC. Conduction are found to decrease with the increase in PbO concentration from 0.3 to 0.7 mol% and then increase for 0.8 and 0.9 PbO mol% indicating an increase in the concentration of Pb^{2+} ions that act as modifiers.

References

[1] Cheng, Y., Xiao, H., & Guo, W. (2007). *Ceram. Inter.*, *33*, 1345.
[2] Dahiya, M. S., Khasa, S., & Agarwal, A. (2015). *J. Molec. Str.*, *1086*, 176.
[3] Abbas, L., Bih, L., Nadiri, A., & El Amraoui, Y. (2008). *J. Molec. Str.*, *876*, 195–197.
[4] Naga, G., Srinivasa, M., Sudhakar, K., & Veeraiah, N. (2007). *Opt. Mater.*, *29*, 1468.
[5] Pascuta, P., Rada, S., Borodi, G., Bosca, M., Pop, L., & Culea, E. (2009). *Molec. J. Str.*, *924*, 218.
[6] Dubois, B., Videau, J. J., Couzi, M., & Portier, J. (1986). *J. Non-Cryst. Solids*, *88*, 355..
[7] Saitoh, A., Tricot, Gr. E., Rajbhandari, P., Anan, S., & Takebe, H. (2014). *J. Mater. Chem. Phys.*, 1.
[8] Mroczkowska, M., Czeppe, T., & Nowinski, J. L. (2008). *Solid State Ionics*, *179*, 202.
[9] Erdogan, C., Bengisu, M., & Erenturk, A. (2014). *J. Nucl. Mater.*, *445*, 157.
[10] Doweidar, H., El-Damrawi, G., & Agammy, E. (2014). *Vibrat. Spectr.*, *73*, 91.
[11] Alajerami, Y., Hashim, S., Hassan, W., & Ramli, A. (2012). *J. Molec. Str.*, *1026*, 162.
[12] Karan, N. K., Natesan, B., & Katiyar, R. S. (2006). *Solid State Ionics*, *177*, 1436.
[13] Subhadra, M., & Kistaiah, P. (2012). *Vibrat. Spectr.*, *62*, 25.
[14] Edukondalu, A., Sathe, V., Rahman, S., & Kumar, K. (2014). *Physica B*, *438*, 123.
[15] Ganguli, M., & Rao, K. J. (1999). *Solid State Str. Chem.*, *145*, 67.
[16] Knoblochova, K., Ticha, H., Schwarz, J., & Tichy, L. (2009). *Opt. Mater.*, *31*, 897.
[17] Lucacel, R., Marcus, C., Timar, V., & Ardelean, I. (2007). *Solid State Sci.*, *9*, 850.
[18] Ushida, H., Iwadate, Y., & Hattori, T. (2004). *J. Alloys Comp.*, *377*, 167.
[19] Kumar, A. V. R., Rao, Ch. S., Krishna, G. M., Kumar, V. R., & Veeraiah, N. (2012). *J. Molec. Str.*, *1016*, 41.
[20] Morsi, R., & Ibrahiem, S. (2011). *Physica. B*, *406*, 2982.
[21] Ramesh, P., Vijay, R., Srinivasa, P., Suresh, P., Veeraiah, N., & Krishna, D. (2013). *J. Non-Cryst. Solids*, *370*, 21.
[22] Korotkova, T., Karaeva, O., Naberezhnov, A., Rysiakiewichz, E., & Korotkov, L. (2012). *Solid State Comm.*, *152*, 846.
[23] Thomas, S., Sajna, M. S., Nayab, S. k., Gopinath, M., Joseph, C., & Unnikrishnan, N. (2015). *Opt. Mater.*, *39*, 167.
[24] Silalai, N., & Roos, Y. H. (2011). *J. Food Eng.*, *104*, 445.
[25] Thomas, S., George, R., Rathaiah, M., & Venkatramu, V. (2013) *Physica. B*, *431*, 69.
[26] Little, G., Sahaya, G., & Srinivasa, M. (2007). *Physica. B*, *393*, 61.
[27] Yoon, Y., Park, C., Kim, J., & Shin, D. (2012). *Solid State Ionics*, *225*, 638.
[28] Guo, H. W., Wang, X. F., Gong, Y. X., & Gao, N. (2010). *J. Non-Cryst. Solids*, *356*, 2110.
[29] EL-Egili, K., Doweidar, H., & Moustapha Abbas, Y. M. (2003). *Physica. B*, *339*, 237.
[30] Koudelka, L., Mosner, P., Zeyer, M., & Jäger, C. (2003). *J. Non-Cryst. Solids*, *326/327*, 72.
[31] Naresh, V., & Buddhudu, S. (2012). *Ceram. Inter.*, *38*, 2326.
[32] Rao, A., Laxmikanth, C., Rao, B., & Veeraiah, N. (2006). *J. Phys. Chem. Solids*, *67*, 2263.
[33] Rao, D., Baskaran, G., Gandhi, Y., & Veeraiah, N. (2015). *Physica B*, *457*, 119.
[34] Selim, M., & Metwalli, E. (2002). *Mater. Chem. Phys.*, *78*, 98.